

*Ab initio* study of the mechanical and transport properties of pure and contaminated silver nanowires

This article has been downloaded from IOPscience. Please scroll down to see the full text article.

2013 J. Phys.: Condens. Matter 25 325303

(<http://iopscience.iop.org/0953-8984/25/32/325303>)

View [the table of contents for this issue](#), or go to the [journal homepage](#) for more

Download details:

IP Address: 129.6.153.91

The article was downloaded on 15/07/2013 at 14:57

Please note that [terms and conditions apply](#).

# *Ab initio* study of the mechanical and transport properties of pure and contaminated silver nanowires

S Barzilai<sup>1</sup>, F Tavazza and L E Levine

Material Measurement Laboratory, National Institute of Standards and Technology, 100 Bureau Drive, Stop 8553, Gaithersburg, MD 20899, USA

E-mail: [barzilai.shmuel@gmail.com](mailto:barzilai.shmuel@gmail.com)

Received 14 March 2013, in final form 7 June 2013

Published 12 July 2013

Online at [stacks.iop.org/JPhysCM/25/325303](http://stacks.iop.org/JPhysCM/25/325303)

## Abstract

The mechanical properties and conductance of contaminated and pure silver nanowires were studied using density functional theory (DFT) calculations. Several nanowires containing O<sub>2</sub> on their surfaces were elongated along two different directions. All of the NWs thinned down to single atom chains. In most simulations, the breaking force was not affected by the presence of the O<sub>2</sub>, and similar fracture strengths of  $\approx 1$  nN were computed for the pure and impure NWs. When the O<sub>2</sub> became incorporated in the single atom chain, the fracture occurred at the Ag–O bond and a lower fracture strength was found. All of the simulations showed that the impurity interacted with the silver atoms to reduce the electron density in its nearby vicinity. A variety of conductance effects were observed depending on the location of the impurity. When the impurity migrated during the elongation to the thinnest part of the NW, it reduced the conductance significantly, and an  $\approx 1 G_0$  conductance (usually associated with a single atom chain) was calculated for three- and two-dimensional structures. When the impurity was adjacent to the single atom chain, the conductance reduced almost to zero. However, when it stayed far from the thinnest part of the NW, the impurity had only a small influence on the conductance.

(Some figures may appear in colour only in the online journal)

## 1. Introduction

The miniaturization of electronic components is one of the significant cornerstones in the development and improvement of new devices in nanoelectronics. Silver nanowires (NWs) are candidates to serve as conductors in these devices. Understanding the mechanical properties and the mechanisms that control the conductance in atomic-scale wires is important both from a basic science standpoint and for applications in nanoelectronics and nano-devices. Numerous experimental studies [1–16] have been conducted to characterize the mechanical properties and the conductance of silver nanowires during elongation. In these experimental systems, the silver NW is elongated and thinned down to a single atom chain (SAC) in a high vacuum chamber, at  $\approx 4$  K. During wire thinning, the conductance is continuously

measured and it is generally accepted that a conductance of  $1 G_0$  (where  $G_0 = 2e^2/h$ , with  $e$  the electron charge and  $h$  Planck's constant) indicates that part of the NW has thinned to a SAC. To validate this interpretation, many theoretical studies have investigated both the structural changes that occur during elongation of silver, gold and copper NWs, and the conductance of these configurations [17–34]. It was found that the arrangement of the metallic atoms changes, during elongation, from three-dimensional (3D) phases to a variety of two-dimensional (2D) phases and finally to a SAC. These simulations show that when part of the NW becomes a SAC, the conductance goes to  $\approx 1 G_0$ . However, in the experiments, contaminants can be adsorbed on the initial NW surface, and migrate during the elongation to the transmission pathway and affect the conductance of the elongated NW. It is well known that the conductance is affected when impurities are pre-placed directly on the SAC [35–51]. Experimental and theoretical studies [14–16, 35–38] show that when O<sub>2</sub> is

<sup>1</sup> On sabbatical leave from the Nuclear Research Center Negev.

introduced to a SAC of silver, the conductance can decrease well below  $1 G_0$ . However, the ability of the  $O_2$  to migrate from the surface of the 3D NWs to the region of the SAC during the elongation, and the effect of the  $O_2$  on the conductance in the 3D and the 2D intermediate structures are still unknown.

To study the effect of an  $O_2$  attached to the silver NW surface on the structural, mechanical and conductance evolution during elongation, we simulate deformation of several silver NWs containing  $O_2$  attached to the surface.

## 2. Methodology

Pure Ag NWs containing 115 atoms oriented with (110) planes perpendicular to the original wire ( $Z$ ) axis, and contaminated silver NWs having the same orientation, were elongated along two directions,  $[19\ 21\ 2]$  and  $[1\ 3\ 2]$ , which are  $6^\circ$  and  $48^\circ$  off the  $Z$  axis. Previous studies in Au [17, 29] examined several tensile axes, both along the high symmetry direction ( $z$ -axis) and forming a small angle with it ( $\approx 1^\circ$ – $5^\circ$  with respect to the  $z$ -axis). In those studies, no significant difference was found in the evolution of the wire except for the exact  $[1\ 1\ 0]$  case for the (110) NW. We believe that in real experiments the alignment between the elongation grips is never perfect, and, therefore, specimens are elongated under small distortions. To introduce such small distortions in our simulations, we choose to elongate the wire along an arbitrary axis  $6^\circ$  off the  $z$  axis. The  $[1\ 3\ 2]$  direction (forming a  $48^\circ$  angle with the  $z$ -axis) was chosen to include the effect of a large lack of symmetry in our simulations. The exact  $[0\ 1\ 1]$  tensile direction was not simulated because earlier work in Au [17] showed anomalous deformation behavior (fracture before a single atom chain was reached) along this axis. This occurred because the high symmetry configuration restricted the available deformation paths.

The (110) orientation has been shown previously [29] to be a preferred orientation, since it transforms into many stable intermediate configurations during the elongation. In contrast, the (111) orientation exhibits a less complicated energy landscape during deformation, giving rise to less varied intermediate configurations. Because of these results, we chose the (110) orientation for this investigation, to increase the statistics of the conductance computation versus atomic configurations. For all simulations, the initial wire configuration was carved out of an ideal fcc lattice with the proper orientation. At each tensile step, the grip atoms (two layers at each end) were translated by a fixed amount, then kept fixed in their fcc positions, while the other atoms were allowed to relax into a new configuration. To determine which impurity sites to investigate, an  $O_2$  molecule was placed on eight different sites on the ideal NWs surface. The contaminated wire was then relaxed and a lowest energy criterion was used to select two sites near the central region of the NW and two sites near the shoulder, adjacent to the rigid grip layers, for the tensile simulations. Figure 1 shows the silver NW and the eight sites that were individually examined.

The simulated elongations of the nanowires were conducted in the framework of density functional theory

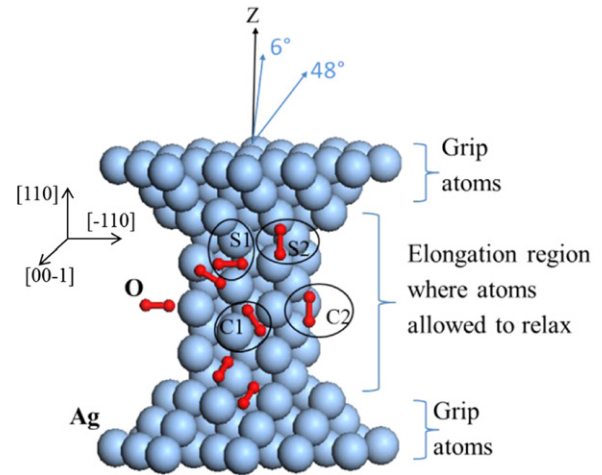


**Figure 1.** Schematic configuration of the silver NW having eight oxygen molecules spread on the surface prior to the relaxation. The encircled molecules were selected for the tensile simulations. The upper two molecules are considered as a shoulder (S1 and S2) type contamination and the lower two encircled molecules are considered as a center type (C1 and C2).

(DFT) using the DMol<sup>3</sup> code [52, 53]<sup>2</sup>. DMol<sup>3</sup> employs localized basis sets, which makes calculations fast and particularly well suited for cluster calculations. We used a double-zeta, atom-centered basis set (dnd) and a real-space cutoff of 4 Å. The exchange–correlation potential was treated within the Perdew–Burke–Ernzerhof (PBE) generalized gradient approximation (GGA) approach [54]. The Ag-ion core electrons were described by a hardness conserving semilocal pseudopotential (dspp) [55], and only the outer electrons ( $4s^2 4p^6 4d^{10} 5s^1$ ) were treated as valence electrons. To allow meaningful comparisons, identical conditions were employed for all systems. A conjugate gradient approach based on a delocalized internal coordinate scheme [56, 57] was used for geometry optimization. The system was considered converged when change in total energy and the atomic displacements dropped below  $10^{-4}$  eV for self-consistent calculations,  $10^{-4}$  Å for maximum displacement and  $10^{-3}$  eV for energy change.

The zero bias conductance calculations were performed with the ATK package [23, 59, 60], using a non-equilibrium Green's function technique based on the Landauer formalism [58]. The system was separated into three regions: the upper and lower Ag electrodes that were attached to the grip atoms (see figure 1) and the central scattering region. For the central region, we used atomic configurations obtained by the DFT elongation. The electrodes were carved out of an ideal Ag face-centered cubic (fcc) lattice with the same orientation as the wire, and were large enough not to constrict the conductance in any way. The electrodes attached seamlessly to the scattering zone since the grip atoms in the deformation simulations were kept fixed in ideal fcc positions. Huckel tight binding [61] was utilized

<sup>2</sup> Commercial software is identified to specify procedures. Such identification does not imply recommendation by the National Institute of Standards and Technology.

**Table 1.** Mechanical characterization and conductance properties of pure and impure silver NWs.

Simulation No.	O <sub>2</sub> location (tensile direction—deviation from Z axis)	Fracture strength <sup>a</sup> (nN)	Fracture strain <sup>b</sup> (%)	The minimal conductance <sup>c</sup> ( $G_0$ )	The maximal chemical effect <sup>d</sup> ( $G_0$ )		
					3D	2D	SAC
1	Pure (6°)	1.00	73	0.98	—	—	—
2	Pure (48°)	1.05	120	0.94	—	—	—
3	Center 1 (6°)	1.02	61	0.67	1.17	0.15	0.20
4	Center 2 (6°)	1.02	130	0.65	0.97	0.16	0.03
5	Shoulder 1 (6°)	0.96	88	0.45	0.77	0.4	0.49
6	Shoulder 2 (6°)	0.90	100	0.73	0.81	0.64	0.22
7	Center 1 (48°)	0.84 <sup>e</sup>	130	0.01	0.86	0.58	0.97
8	Center 2 (48°)	0.90	141	0.69	0.88	0.63	0.25
9	Shoulder 1 (48°)	0.89	164	0.86	0.56	0.07	0.03
10	Shoulder2 (48°)	1.03	109	0.88	0.70	0.01	0.07

<sup>a</sup> The fracture strength was computed by dividing the difference between the total energy of the NW at the iteration of the breakage and the previous one, by the change in the NW length caused by this step.

<sup>b</sup> The engineering strain computed by dividing the change of the NW length by the initial length of the elongation region.

<sup>c</sup> The minimum conductance that was calculated for the NW during the elongations. These value correspond to the SAC phase.

<sup>d</sup> The maximal conductance difference between the NW that includes the impurity and the identical NW structure without the impurity.

<sup>e</sup> The fracture took place on the Ag–O bond.

for all of the cluster-based configurations (retrieved from the DFT simulations) using the Cerda [62] and Hoffmann [63] parameterization for the Ag and for the O atoms, respectively.

### 3. Results

Pure and contaminated silver NWs were elongated along directions 6° and 48° off the wire axis. To estimate the fracture strength of the silver NWs, we divided the change in total energy between the last two steps, by the corresponding change in the NW length. In previous studies on gold NWs [17, 64], this methodology provided a good agreement with the experimental value observed by Rubio-Bollinger *et al* [65]. While no experimental data are available for silver NWs, the fracture results of 1.00 nN and 1.05 nN obtained here for pure silver NWs are in a good agreement with the computed results of 0.9 nN [66] and 1.06 nN [37] reported in the literature. In all but one of the simulations of contaminated NWs (see table 1), the O<sub>2</sub> did not incorporate into the SAC during the elongation even though it changed orientation relative to the silver atoms. In these cases, the fractures occur at an Ag–Ag bond resulting in a fracture strength and its standard deviation of  $(0.96 \pm 0.06)$  nN which coincide, within the uncertainties, with the available results for pure NWs. In the only case when the O<sub>2</sub> was incorporated into the SAC at the final stages of the elongation, the fracture took place at the Ag–O bond and a lower fracture strength of 0.84 nN was computed.

The fracture strain is computed by dividing the total change of the NW length by the initial length of the elongation region. In most of the simulations, the presence of the O<sub>2</sub> increased this strain as compared with pure NWs (see table 1). This increase was also observed experimentally by Thijssen *et al* [14, 15] when oxygen was admitted to pure silver nanowires.

Figure 2 shows the computed conductance as a function of elongation for three representative simulations of the

contaminated NWs. Snapshots from these elongations are presented at the bottom of the figure. The simulation results demonstrate that the presence of an O<sub>2</sub> molecule always has some effect on the conductance of the NWs because its presence causes ‘chemical’ interactions and dictates structural changes. To separate these effects, the conductance of each elongated NW was calculated at every elongation step both with the impurity (solid symbols) and with the impurity removed (hollow symbols). When the impurity is removed, no structural relaxations are carried out and identical configurations of the silver atoms were considered. These structures are different from those observed during the elongation of pure silver NWs but they allow the ‘chemical’ contribution of the impurity to be evaluated. The remaining simulations are summarized in table 1 and exhibit similar impurity effects to those shown in figure 2. Prior to the elongation, all the simulations show that the adsorption of an O<sub>2</sub> on the NW surface reduces the conductance by 0.5  $G_0$  to 0.9  $G_0$ , depending on its location. During the elongation, two kinds of effects due to the O<sub>2</sub> were observed. First, a small decrease in the conductance was found for the silver NWs that thinned down far from the contaminant. This decrease only occurred in the early stages of the elongation and was almost undetectable afterward, when the structural changes of the silver atoms dictate and limit the conductance. A representative simulation with this behavior is shown in figure 2(a). When the thinning process occurs near the O<sub>2</sub>, the O<sub>2</sub> interacts with the silver atoms that are in the main transmission pathway, and decrease the conductance by a substantial amount as long as the contaminant remains adjacent to the thinned out region. In figure 2(b), the O<sub>2</sub> is near the thinning zone until part of this area evolves into a SAC. Up to that point, the presence of the O<sub>2</sub> decreases the conductance by 0.3  $G_0$  to 0.9  $G_0$ . Moreover, the conductance of 1  $G_0$  that experimentalists use it as an indication of the presence of a SAC during tensile experiments, was found for a much thicker NW (see insets C, D in figure 2(b)). Figure 2(c)

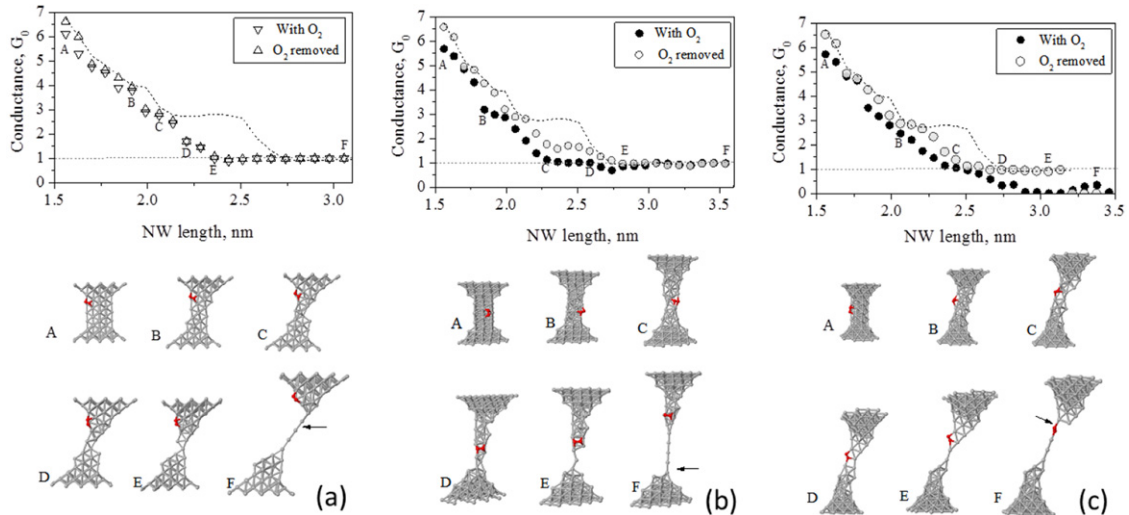


**Figure 2.** The computed conductance of representative silver NWs during elongation. The solid symbols represent the presence of an  $O_2$  impurity on the surface of the NW. The hollow symbols refer to the same atomic configuration of the silver atoms, but without the oxygen, the dashed line refers to the pure Ag NW that was elongated without the presence of the  $O_2$ . The arrows indicate the fracture location.

presents results for the case where the final stage of thinning down to a SAC took place near the  $O_2$ . In this case, the conductance drops well below 1 (figure 2(c)) as soon as the  $O_2$  is attached to the SAC (configuration D in figure 2(c)) and remains extremely low when it is incorporate into it. These low levels of conductance were experimentally observed by Thijssen *et al* [14], when  $O_2$  was admitted into the chamber during silver NW elongation. It is worth mentioning that at the end of the elongation, when the NWs become SACs, small conductance oscillations were observed for both the pure and the contaminated NWs. This phenomenon has been explained by the resonant transport model [67–69] by Kwapiński and Thygesen *et al*.

To better understand the effect of the  $O_2$  on the conductance of silver NWs, the electronic properties were analyzed for a variety of contaminated NWs and compared to the same NWs configurations after removing the  $O_2$ . A generic electronic behavior was obtained for the cases where the presence of  $O_2$  significantly decreased the conductance and for the cases where it hardly affected the conductance. The transmission pathways (figure 3) and the electron density (figure 4) are discussed here using the atomic configurations shown in figure 2(c)-E and in figure 2(b)-F as representative situations for these cases.

For the atomic configuration in figure 2(c)-E ( $O_2$  adjacent to the SAC region), the transmission path was computed with the  $O_2$  (figure 3(a)) and after removing the  $O_2$  (figure 3(b)). Significant changes took place between the two cases, including in the local conductance between the Ag–Ag pairs of atoms. As can be seen in figure 3(c), very small local currents were computed when the  $O_2$  was adjacent to the SAC (the dark area of the figure) while a significant increase in such currents was found when the  $O_2$  was removed. Very different effects were obtained for  $O_2$  located on a thicker part of the NW, away from the SAC (as in the configuration in figure 2(b)-F). Here, the main transmission pathway was hardly affected by the presence of the  $O_2$  (figures 3(d) and

(e)) and very similar local currents were obtained for the case with the  $O_2$  and after removing it (figure 3(f)). The conduction channels that fed the main transmission got thinner near the  $O_2$  compared to the results obtained after removing the oxygen. To compensate for this current depletion, other channels, far from the  $O_2$ , increased their capacity to feed the SAC conductance bottleneck (see arrows in figure 3(d) and the inset in figure 3(f)) and preserved a similar total conductance.

The effects of the  $O_2$  on the local electron density are shown in figure 4. Here, an increase is defined as the increase of the electron density relative to the individual atoms. For both configurations, the  $O_2$  depletes the electron density in its vicinity. Despite this similarity, the depletion has different effects on the conductance. When the impurity is near the thin region of the NW (as in figure 4(a)), the electron depletion decreases the availability of the electrons in the bottleneck of the transmission path. In this case, the presence of the  $O_2$  decreases the conductance from  $\approx 0.9 G_0$  to  $\approx 0.01 G_0$ . However, when the  $O_2$  is located near a thicker region (as in figure 4(c)), the electron depletion caused by the  $O_2$  is concentrated in this local region and does not reach to the thinner part of the NW (see the differences between figures 4(c) and (d)). In this case, the conductance is dictated by the atomic configuration of the thinnest part of the NW, and the presence of the  $O_2$  does not affect it.

#### 4. Summary and conclusions

Pure and impure silver NWs were elongated along two different directions. Prior to the elongation,  $O_2$  molecules were placed and relaxed on several locations on the silver NW surface, to study the effect of  $O_2$  contaminants on the mechanical and conductance properties. All of the simulations showed that the NW thins down to a SAC during elongation before the breaking. When the fracture occurred by breaking an Ag–Ag bond, the fracture strength of the pure and the

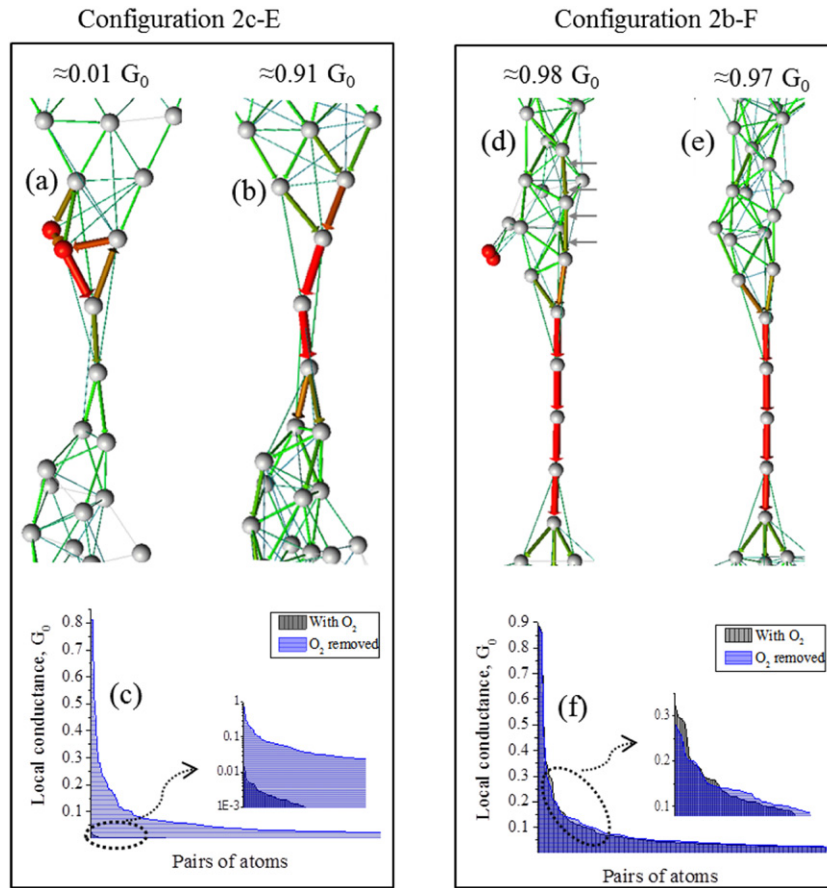


**Figure 3.** Transmission pathways at the Fermi level for representative configurations where the O<sub>2</sub> impurity is adjacent to the thin part of the NW (a) and for the same configuration but after removing the O<sub>2</sub> (b). (c) Corresponds to the calculated local conductance between pairs of atoms for these cases. (d)–(f) provide the corresponding results for the case where the O<sub>2</sub> impurity is adjacent to a thicker part of the NW. The thickness and the colors of the arrows are related to level of the local conductance between each pair of atoms and are normalized to the maximal value in each figure.

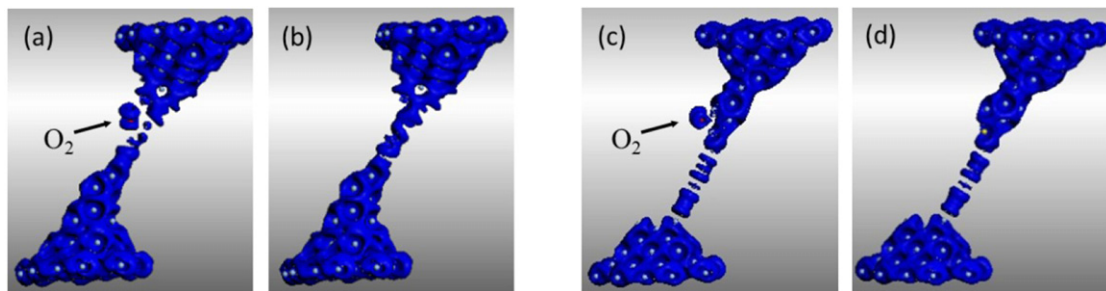


**Figure 4.** The iso-surface of an electron density increase by  $5 \times 10^{-3} \text{ e}^{-3} \text{ \AA}^{-3}$ , corresponding to two different configurations observed during the elongation of contaminated silver NWs. (a) The O<sub>2</sub> impurity adjacent to the thin part of the NW (configuration 2c-E in figure 2). (b) the same configuration as in (a) but after removing the O<sub>2</sub>. (c) The O<sub>2</sub> impurity adjacent to a thicker part of the NW (configuration 2b-F in figure 2) and (d) the same configuration as in (c) but after removing the O<sub>2</sub>.

impure NWs gave similar results. However, when the O<sub>2</sub> was incorporated into the SAC, the fracture took place in the Ag–O bond and the fracture strength was lower by  $\approx 12\%$ .

All of the simulations showed that the O<sub>2</sub> impurity interacts with the silver atoms to reduce the local electron density. This depletion reduces the conductance by  $0.3 G_0$  to  $0.9 G_0$  if the oxygen is located close to the thinnest part of the NW, which acts as a bottleneck for electron

transmission. For these situations, and in a good correlation with the experimental results of Thijssen *et al* [14], the conductance decrease caused by the oxygen at the late stages of the elongation resulted in almost a zero conduction when the oxygen was adjacent to the SAC region. However, for the intermediate thicker structures observed during the elongation, when the oxygen was near the thin part of the NW and before it transform to SAC, the conductance decreased to

$\approx 1 G_0$  even for 3D atomic configurations. In most NW tensile experiments, this level of conductance is used to indicate that part of the NW transforms to a SAC. However, as it was demonstrated in the present simulations, this conductance can also be achieved by contamination of a 3D or 2D NW structure. A different effect was found when the impurities were a little farther from the thinnest part of the NWs. The conductance channels in the thicker parts are used to feed the main transmission pathway and utilize only small part of their available capacity. In these cases, when the  $O_2$  depletes the electrons from the channels in its nearby location, other conduction channels compensate by increasing their conduction. Thus, when the  $O_2$  is located away from the thinnest part of the NW, the conductance is hardly changed.

## References

- [1] Yanson I K, Shklyarevskii O I, Csonka Sz, van Kempen H, Speller S, Yanson A I and van Ruitenbeek J M 2005 *Phys. Rev. Lett.* **95** 256806
- [2] Kiguchi M, Konishi T and Murakoshi K 2006 *Phys. Rev. B* **73** 125406
- [3] Kiguchi M, Konishi T, Tasegawa K, Shidara S and Murakoshi K 2008 *Phys. Rev. B* **77** 245421
- [4] Kiguchi M, Djukic D and van Ruitenbeek J M 2007 *Nanotechnology* **18** 035205
- [5] Suzuki R, Tsutsui M, Miura D, Kurokawa S and Sakai A 2007 *Japan. J. Appl. Phys.* **46** 3694
- [6] Kizuka T 2008 *Phys. Rev. B* **77** 155401
- [7] Oshima Y, Kurui Y and Takayanagi K 2010 *J. Phys. Soc. Japan* **79** 054702
- [8] Scheer E et al 1998 *Nature* **394** 154
- [9] Kurui Y, Oshima Y, Okamoto M and Takayanagi K 2009 *Phys. Rev. B* **79** 165414
- [10] Smit R H M, Untiedt C, Rubio-Bollinger G, Segers R C and van Ruitenbeek J M 2003 *Phys. Rev. Lett.* **91** 076805
- [11] Dreher M, Pauly F, Heurich J, Cuevas J C, Scheer E and Nielaba P 2005 *Phys. Rev. B* **72** 75435
- [12] Ohnishi H, Kondo Y and Takayanagi K 1998 *Nature* **395** 780
- [13] Smith D T, Pratt J R, Tavazza F, Levine L E and Chaka A M 2010 *J. Appl. Phys.* **107** 084307
- [14] Thijssen W H A, Marjenburgh D, Bremmer R H and van Ruitenbeek J M 2006 *Phys. Rev. Lett.* **96** 026806
- [15] Thijssen W H A, Strange M, de Brugh J and van Ruitenbeek J M 2008 *New J. Phys.* **10** 33005
- [16] Boer den D et al 2011 *J. Phys. Chem. C* **115** 8295
- [17] Tavazza F, Levine L E and Chaka A M 2009 *J. Appl. Phys.* **106** 43522
- [18] Agraít N, Yeyati A L and van Ruitenbeek J M 2003 *Phys. Rep.* **377** 81
- [19] Agraít N, Rubio G and Vieira S 1995 *Phys. Rev. Lett.* **74** 3995
- [20] Rubio-Bollinger G, Joyez P and Agraít N 2004 *Phys. Rev. Lett.* **93** 11680
- [21] Nitzan A and Ratner M A 2003 *Science* **300** 1384
- [22] Qian Z, Li R, Hou S, Xue Z and Sanvito S 2007 *J. Chem. Phys.* **127** 194710
- [23] Brandbyge M, Mozoz J L, Ordejon P, Taylor J and Stokbro K 2002 *Phys. Rev. B* **65** 165401
- [24] Fujimoto Y and Hirose K 2003 *Phys. Rev. B* **67** 195315
- [25] Lee Y J et al 2004 *Phys. Rev. B* **69** 125409
- [26] Zhuang M and Ernzerhof M 2004 *J. Chem. Phys.* **120** 4921
- [27] Ke L et al 2007 *Nanotechnology* **18** 095709
- [28] Grigoriev A, Skorodumova N V, Simak S I, Wendin G, Johansson B and Ahuja R 2006 *Phys. Rev. Lett.* **97** 236807
- [29] Tavazza F, Levine L E and Chaka A M 2010 *Phys. Rev. B* **81** 235424
- [30] Tavazza F, Smith D T, Levine L E, Pratt J R and Chaka A M 2011 *Phys. Rev. Lett.* **107** 126802
- [31] Szczesniak D and Khater A 2012 *Eur. Phys. J. B* **85** 174
- [32] Kwapinski T 2010 *J. Phys.: Condens. Matter* **22** 295303
- [33] Shiota T, Mares A I, Valkering A M C, Oosterkamp T H and van Ruitenbeek J M 2008 *Phys. Rev. B* **77** 125411
- [34] Rubio-Bollinger G, de las Heras C, Bascones E, Agraít N, Guinea F and Vieira S 2003 *Phys. Rev. B* **67** 12140
- [35] Qi Y, Guan D, Jiang Y, Zheng Y and Liu C 2006 *Phys. Rev. Lett.* **97** 256101
- [36] Strange M, Thygesen K S, Sethena J P and Jacobson K W 2008 *Phys. Rev. Lett.* **100** 96804
- [37] Çakir D and Gülseren O 2011 *Phys. Rev. B* **84** 85450
- [38] Ishida H 2007 *Phys. Rev. B* **75** 205419
- [39] Novaes F D, da Silva A J R, da Silva E Z and Fazzio A 2006 *Phys. Rev. Lett.* **96** 016104
- [40] da Silva E Z, Novaes F D, da Silva A J R and Fazzio A 2006 *Nanoscale Res. Lett.* **1** 91
- [41] Ishida H 2008 *Phys. Rev. B* **77** 155415
- [42] Skorodumova N V and Simak S I 2003 *Phys. Rev. B* **67** 121404R
- [43] Skorodumova N V, Simak S I, Kochetov A E and Johansson B 2007 *Phys. Rev. B* **75** 235440
- [44] Legoas S B, Rodrigues V, Ugarte D and Galvao D S 2004 *Phys. Rev. Lett.* **93** 216103
- [45] Velez P, Dassie S A and Leiva E P M 2010 *Phys. Rev. B* **81** 125440
- [46] Hobi E Jr, Fazzio A and da Silva A J R 2008 *Phys. Rev. Lett.* **100** 056104
- [47] Kochetov A E and Mikhaylushkin A S 2008 *Eur. Phys. J.* **61** 441
- [48] Zhang C, Barnett R N and Landman U 2008 *Phys. Rev. Lett.* **100** 046801
- [49] Barnett R N, Hkkinen H, Scherbakov A G and Landman U 2004 *Nano Lett.* **4** 1845
- [50] Bahn S R, Lopez N, Norskov J K and Jacobsen K W 2002 *Phys. Rev. B* **66** 081405 R
- [51] Jelínek P, Prez R, Ortega J and Flores F 2008 *Phys. Rev. B* **77** 115447
- [52] Delley B 1990 *J. Chem. Phys.* **92** 508
- [53] Delley B 2000 *J. Chem. Phys.* **113** 7756
- [54] Perdew J P, Burke S and Ernzerhof M 1996 *Phys. Rev. Lett.* **77** 3865
- [55] Delley B 2002 *Phys. Rev. B* **66** 155125
- [56] Pulay P and Fogarasi G 1992 *J. Chem. Phys.* **96** 2856
- [57] Baker J, Kessi A and Delley B 1996 *J. Chem. Phys.* **05** 192
- [58] Datta S 1995 *Electron Transport in Mesoscopic Systems* (Cambridge: Cambridge University Press)
- [59] *Atomistix ToolKit Version 10.02* QuantumWise A/S
- [60] Taylor J, Guo H and Wang J 2001 *Phys. Rev. B* **63** 245407
- [61] Stokbro K et al 2010 *Phys. Rev. B* **82** 075420
- [62] Cerda J and Soria F 2000 *Phys. Rev. B* **61** 7965
- [63] Ammeter J H, Burgi H B, Thibeault J C and Hoffmann R 1978 *J. Am. Chem. Soc.* **100** 3686
- [64] Barzilai S, Tavazza F and Levine L E 2013 *Modelling Simul. Mater. Sci. Eng.* **21** 25004–1
- [65] Rubio-Bollinger G, Bahn S R, Agraít N, Jacobsen K W and Vieira S 2001 *Phys. Rev. Lett.* **87** 26101
- [66] Bahn S R and Jacobsen K W 2001 *Phys. Rev. Lett.* **87** 266101
- [67] Thygesen K S and Jacobsen K W 2003 *Phys. Rev. Lett.* **91** 146801
- [68] Kwapiński T K 2005 *J. Phys.: Condens. Matter* **17** 5849
- [69] Kwapiński T K 2007 *J. Phys.: Condens. Matter* **19** 176218